



## Fracture mechanics of non-shear reinforced R/C Beams

Kerelezova, Irina; Hansen, Thomas; Nielsen, Mogens Peter

*Publication date:*  
2007

*Document Version*  
Publisher's PDF, also known as Version of record

[Link back to DTU Orbit](#)

*Citation (APA):*  
Kerelezova, I., Hansen, T., & Nielsen, M. P. (2007). *Fracture mechanics of non-shear reinforced R/C Beams*. Byg Rapport No. R-154 <http://www.byg.dtu.dk/upload/institutter/byg/publications/rapporter/byg-r154.pdf>

---

### General rights

Copyright and moral rights for the publications made accessible in the public portal are retained by the authors and/or other copyright owners and it is a condition of accessing publications that users recognise and abide by the legal requirements associated with these rights.

- Users may download and print one copy of any publication from the public portal for the purpose of private study or research.
- You may not further distribute the material or use it for any profit-making activity or commercial gain
- You may freely distribute the URL identifying the publication in the public portal

If you believe that this document breaches copyright please contact us providing details, and we will remove access to the work immediately and investigate your claim.

Irina Kerelezova  
Thomas Hansen  
M. P. Nielsen

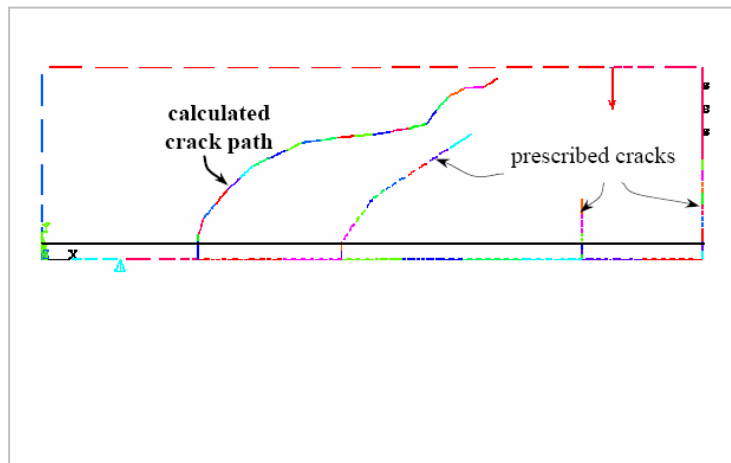
## Fracture Mechanics of Non-Shear Reinforced R/C Beams

Report  
BYG·DTU  
R-154  
2007

ISSN 1601-2917  
ISBN 97887-7877-226-5

# Fracture Mechanics of Non-Shear Reinforced R/C Beams

Irina Kerelezova  
Thomas Hansen  
M. P. Nielsen



Department of Civil Engineering  
DTU-bygning 118  
2800 Kgs. Lyngby  
<http://www.byg.dtu.dk>

2007

# FRACTURE MECHANICS OF NON-SHEAR REINFORCED R/C BEAMS

Irina Kerelezova<sup>1</sup>, Thomas Hansen<sup>2</sup> and M. P. Nielsen<sup>3</sup>

## ABSTRACT

A fracture mechanics analysis of the shear strength of non-shear reinforced concrete beams is carried out.

The starting point of the shear crack is determined by means of the crack sliding theory. The crack path is determined by using the principal stress conditions of linear fracture mechanics. Crack growth is calculated by a theoretical crack growth formula. The formula is based on a non-linear two parameter fracture mechanics model and gives a possibility to investigate the full crack development.

The numerical simulations are carried out using APDL (ANSYS Parameter Design Language) programming language of the finite element package ANSYS.

The calculations seem to indicate that the final shear failure in the beams treated is not a fracture mechanics problem. If this is a general trend is not yet clear. More calculations have to be carried out.

---

<sup>1</sup> Assistant professor, Dr., Eng., Department of Structural Engineering, University of Architecture, Civil Engineering and Geodesy; Bulgaria; **e-mail: igk\_fce@uacg.bg**

<sup>2</sup> Civil Engineer, M. Sc., PhD. Student, Birch & Krogboe A/S, Consultant and Planners; **e-mail: tmh@birch-krogboe.dk**

<sup>3</sup> Professor Emeritus, Dr. techn., BYG•DTU, Technical University of Denmark; **e-mail: mpn@byg.dtu.dk**

# 1 THE SHEAR CRACK PROBLEM

From experiments, it is a well-known fact that the shear crack path depends on the size of the beam and on the shear span ratio. The critical shear crack can be an almost straight line, a curved line, or in some cases beams collapse without forming a critical shear crack. The position of the critical shear crack is also different and dependent on many parameters.

In this paper the position of the critical shear crack is predicted using the crack sliding theory [1]. Jin-Ping Zhang deduced the following criterion:

$$f_c^* \left( \sqrt{1 + \left( \frac{a-x}{h} \right)^2} - \frac{a-x}{h} \right) = f_t^* \frac{1 + \left( \frac{a-x}{h} \right)^2}{\frac{a}{h} + \frac{L_0}{2h}}, \quad (1)$$

Here  $f_c^*$  is the effective compressive strength of concrete,  $f_t^*$  is the equivalent effective tensile strength,  $L_0$ ,  $h$ ,  $x$  and  $a$  are geometrical parameters and may be seen in Figure 1.

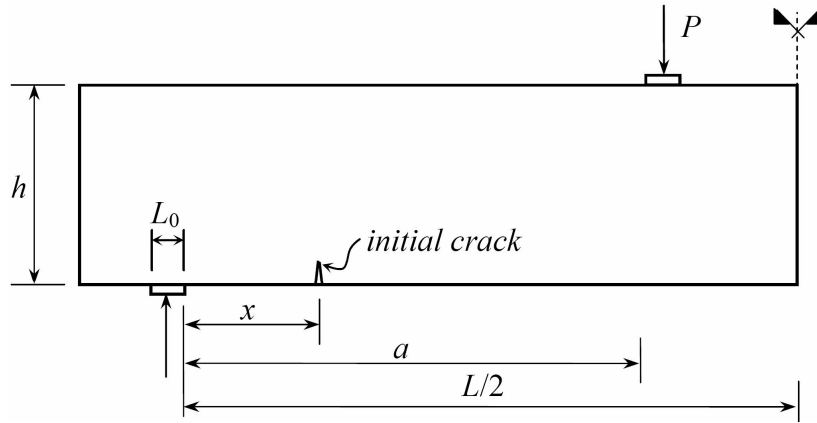


**Figure 1:** Position of the critical shear crack

Crack sliding theory is a theory of plasticity for non-shear reinforced beams. The Jin-Ping Zhang formula is a condition for the equality of cracking load and load-carrying capacity, see Figure 2.

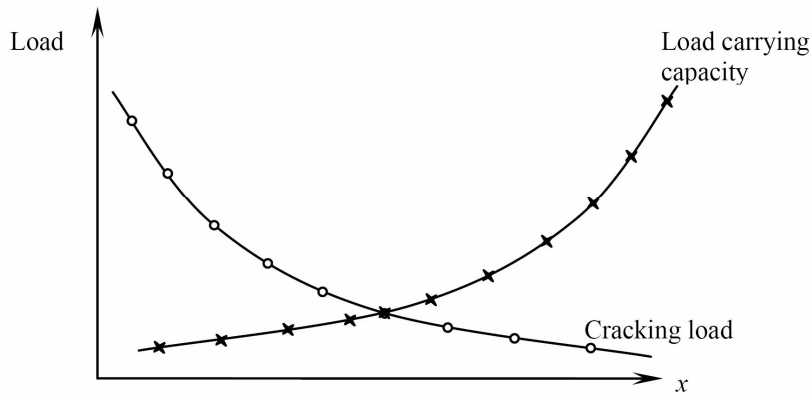


**Figure 2:** Condition for shear failure along critical shear crack

The cracking load is the load needed for formation of an arbitrary shear crack and the load carrying capacity is the load needed for sliding failure through the crack. When these loads are equal failure through a critical shear crack takes place.

One can see from experiments that the crack path of both the critical and the secondary cracks closely follow the orientation of the principal stresses of the beam without cracks. Figure 3 shows the principal stresses in a typical beam and the experimental cracks. The experimental results are taken from [2].

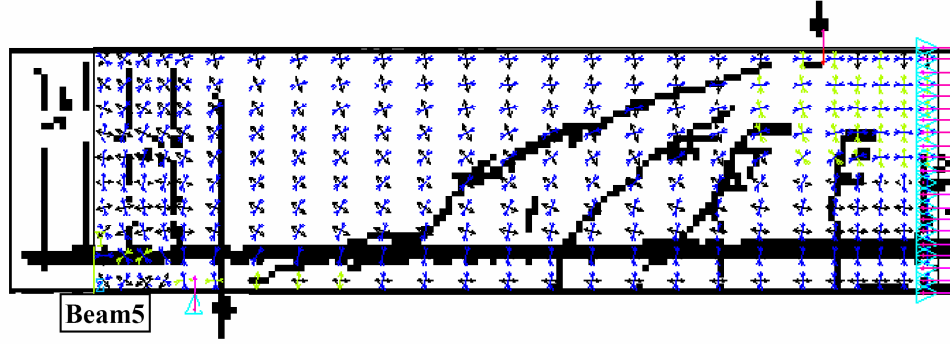


**Figure 3:** Principal stress direction

For this reason, we follow the well-known method from linear elastic fracture mechanics (LEFM), see for instance [4], using the principal stress criterion to determine the crack path of the critical shear crack. This criterion is described by the following equations:

$$\begin{aligned} K_I \cos^2 \frac{\theta_c}{2} \sin \frac{\theta_c}{2} + K_{II} \cos \frac{\theta_c}{2} \left( \cos^2 \frac{\theta_c}{2} - 2 \sin^2 \frac{\theta_c}{2} \right) &= 0, \\ K_I \cos^3 \frac{\theta_c}{2} - 3 K_{II} \cos^2 \frac{\theta_c}{2} \sin \frac{\theta_c}{2} &= K_{Ic}, \end{aligned} \quad (2)$$

Here  $K_I$  and  $K_{II}$  are stress intensity factors for mode I and II, respectively,  $\theta_c$  is the angle between new and present crack direction,  $K_{Ic}$  the critical stress intensity factor for mode I, which is assumed to be a material constant. In these calculations  $K_{Ic}$  was put equal to  $43.8 \text{ N/mm}^{3/2}$ . This value is slightly lower than the value corresponding to the Young's modulus and the fracture energy given below ( $56.8 \text{ N/mm}^{3/2}$ ). It was verified that this difference had only insignificant influence on the calculated crack path.

## 2 THEORETICAL MODEL FOR CRACK GROWTH

In this paper we use the crack growth formula proposed by the third author, cf. [3]. This formula is based on an energy balance equation leading to a simple fracture mechanics model for crack growth of brittle and quasi-brittle materials. The equation reads:

$$\frac{da}{du} = \frac{-\frac{\partial W}{\partial a} \frac{\partial l_e}{\partial u}}{G_F b + \frac{\partial W}{\partial a} \left(1 + \frac{\partial l_e}{\partial a}\right)} \quad (3)$$

This equation is a first order differential equation for the crack length,  $a$ , as a function of the displacement,  $u$ , in a displacement controlled system. In the equation,  $W$  is the strain energy of the system,  $G_F$  the fracture energy, and  $b$  the thickness of the plane model.

The theoretical model is illustrated in Figure 4. Here the physical meaning of the effective length,  $l_e$ , the length of the process zone,  $a_p$ , and the approximate process zone,  $a'_p$ , according the present model, is shown. The coordinate,  $x$ , is measured along the crack,  $f_t$  is the tensile strength and the parameters,  $w_o$  and  $w'$ , are crack opening displacements. The length of the approximate process zone,  $a'_p$ , is obtained by an Irwin type equilibrium calibration. The effective crack length,  $a + l_e$ , has been determined by approximate energy considerations leading to almost the same result as the Irwin crack length correction, see [7].

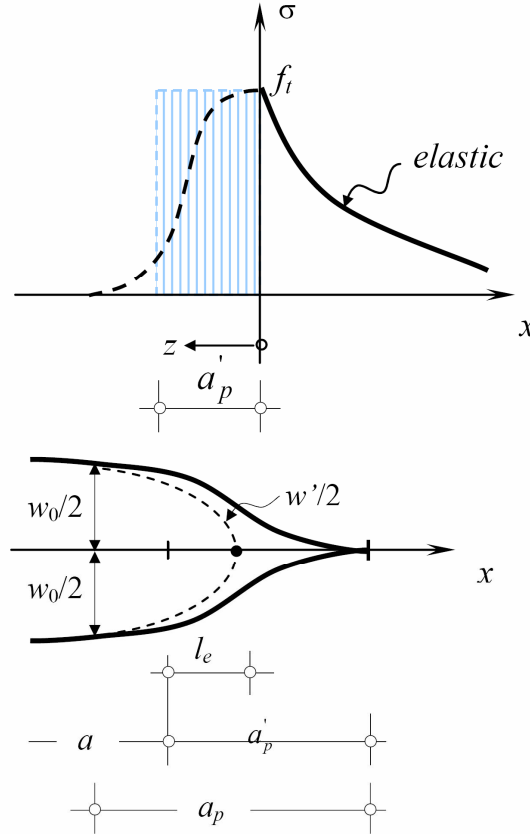


**Figure 4:** The crack growth model

The result from [3] is:

$$l_e = 0.4 a_p' = \frac{0.4 K_I^2}{\pi f_t^2} \quad (4)$$

In the crack growth formula the derivative,  $\partial W/\partial a$ , should be calculated for the effective crack length,  $a + l_e$ .

The model is a simple extension of linear elastic fracture mechanics using two fracture parameters, namely: the tensile strength,  $f_t$ , and the fracture energy,  $G_F$ . The strain energy may be calculated from a series of linear elastic solutions for different crack lengths. The numerical solution of Equation (3) is easily performed using for instance the Runge-Kutta technique.

Regarding the use of (3) in symmetrical crack growth cases (mode I) in plain concrete beams, see [5] and [6].

### 3 NUMERICAL MODEL, RESULTS AND COMPARISONS

The two beams treated have been taken from a test series described in [2]. The beams are named beam 5 and beam 8, respectively. All beams had rectangular section, depth 320 mm and width 190 mm. The reinforcement was 2  $\phi 26$  mm (reinforcement area  $A_s = 1062 \text{ mm}^2$ ). The effective depth was 270 mm.

The average cube strength for all beams was 35 MPa. The tensile strength,  $f_t$ , and the Young's modulus,  $E$ , were not measured in this particular test series. In [5] the tensile strength used in the crack growth formula was 25 % higher than the standard tensile strength, which we shall also follow here. Using traditional empirical formulae, we find that the tensile strength,  $f_t$ , may be set to 3.74 MPa and the Young's modulus to 33700 MPa. For the reinforcement we use the Young's modulus  $2 \cdot 10^5$  MPa.

The loading arrangement was two symmetrical concentrated forces on simply supported beams.

For numerical simulations of the present theory, the finite element program ANSYS is used. First, we need to determine the position of the critical shear crack and the crack path along the beam depth. The critical shear crack position in the bottom face is calculated using Equation (1). The longitudinal reinforcement is linear elastic and modelled with either a spring finite element or with a so-called bar element. The stiffness of the spring was calculated on the basis of empirical formulae for crack spacing. When bar elements were used, the bars were normally anchored in the midpoints between two neighbour cracks with no bond between concrete and steel between the anchor points.

The following results are based on the spring model. To obtain a more realistic modelling of the cracked beam some other prescribed cracks have been added to the beam. Figure 5 shows the model of beam 5.



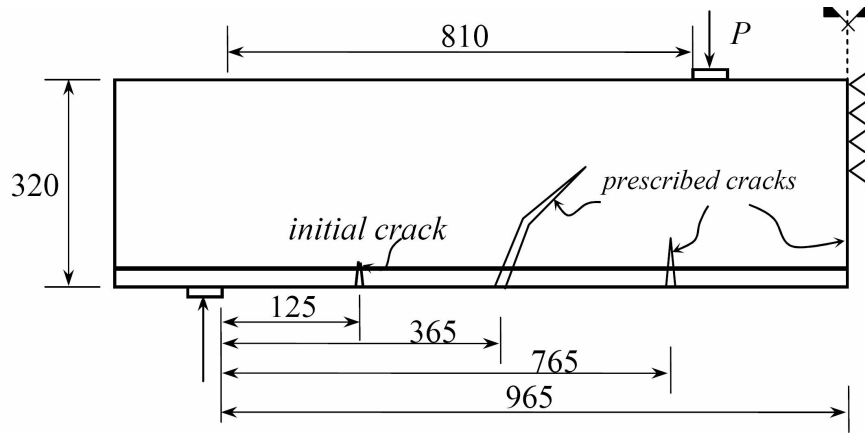


**Figure 5:** Initial position of the critical shear crack for beam 5 and prescribed cracks (measurements in mm)

The reinforcement ratio has a great influence on the crack growth. If the beam is without any reinforcement, the crack grows along an almost vertical line like a bending crack. With increasing reinforcement ratio the crack path becomes more and more curved. In Figures 6 and 7 two cases are shown. The first one (Figure 6) is with reinforcement ratio zero and the second one is with the actual reinforcement,  $A_s = 1062 \text{ mm}^2$ .

The experimental crack pattern for beam 5 is the one shown in Figure 3.

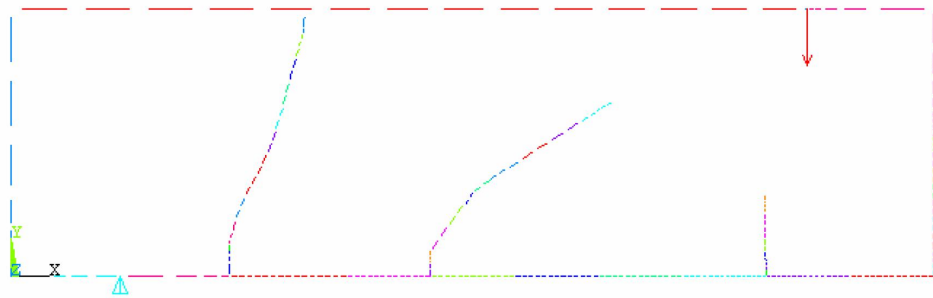


**Figure 6:** Calculated critical shear crack path for beam 5 with no longitudinal reinforcement

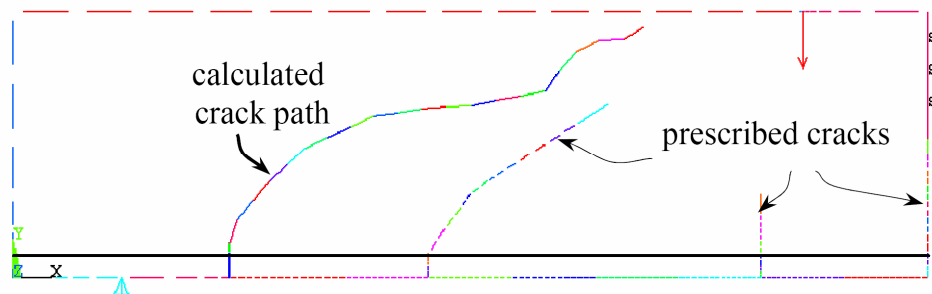


**Figure 7:** Calculated critical shear crack path for beam 5

The next step is calculation of the elastic energy,  $W$ , as a function of the crack length,  $a$ . The APDL (ANSYS Parameter Design Language) programming language of the finite element package ANSYS has been used. These macros calculate elastic strain energy for different crack lengths.

In the experimental data in [2], no information is given for concrete fracture energy. The fracture energy has been taken as  $G_F = 0.0957$  N/mm, a typical value used in [6]. The energy curve, i.e. the elastic energy,  $W$ , for half the beam as a function of the crack length,  $a$ , has been shown in Figure 8 for beam 5.

When the energy curve is known the differential equation, cf. Equation (3), may be solved using the Runge-Kutta technique. This calculation gives us the crack length as a function of the deflection,  $u$ , at the concentrated force. Then the force as a function of  $u$  may be calculated. It should be noticed that when solving Equation (3), the term,  $1 + \partial l_e / \partial a$ , in the denominator has been disregarded.

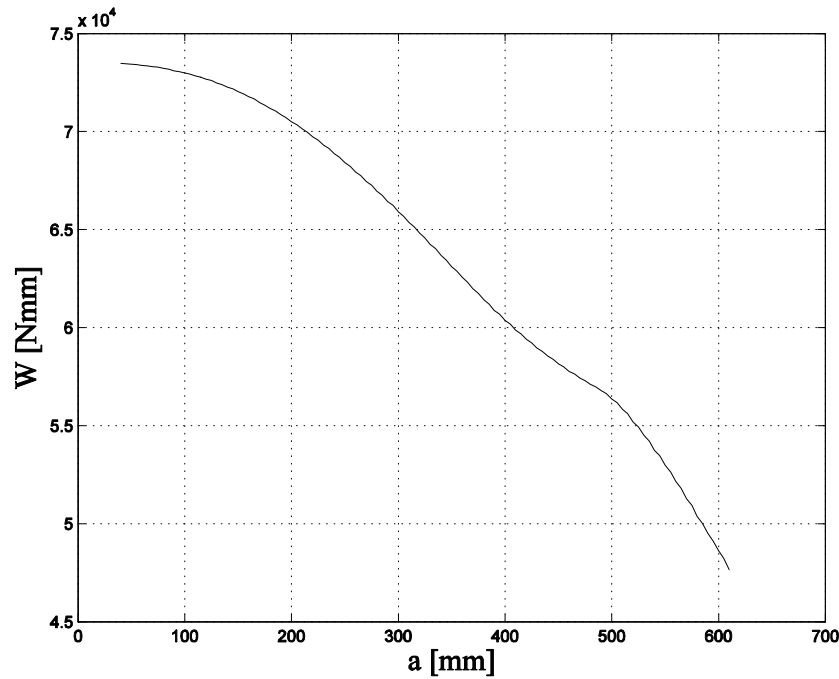


**Figure 8:** Energy,  $W$ , as a function of crack length,  $a$ , for beam 5

Some results for beam 5 with initial crack length 41 mm are shown in the Figures 9 – 14 for 3 different tensile strengths  $f_t = 3.74$  MPa,  $f_t = 2.99$  MPa and  $f_t = 4.49$  MPa. The results are particularly interesting compared to the results in [5] and [6], because after some crack growth the denominator in Equation (3) becomes zero, which means that  $da/du = \infty$ .

Putting the denominator equal to zero is equivalent to the Griffith criterion for unstable crack growth. In regions where the denominator is zero the crack growth is treated as a pure Griffith problem indicated by a dotted line in the figures.

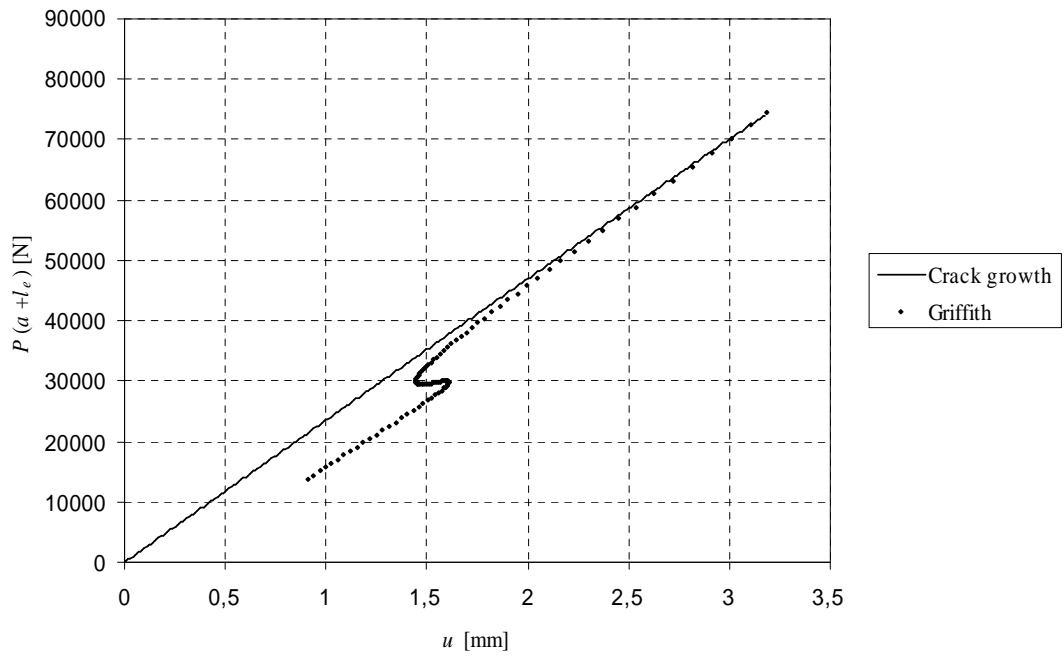


**Figure 9:** Load-deflection curve for beam 5,  $f_t = 3.74$  MPa

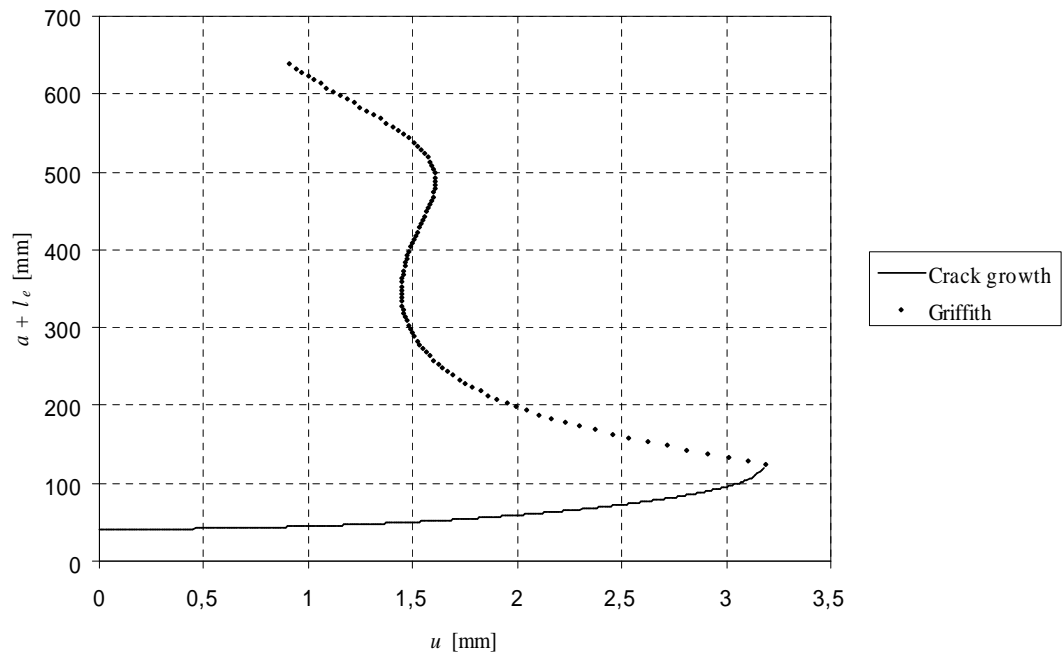


**Figure 10:** Crack length as a function of deflection for beam 5,  $f_t = 3.74$  MPa

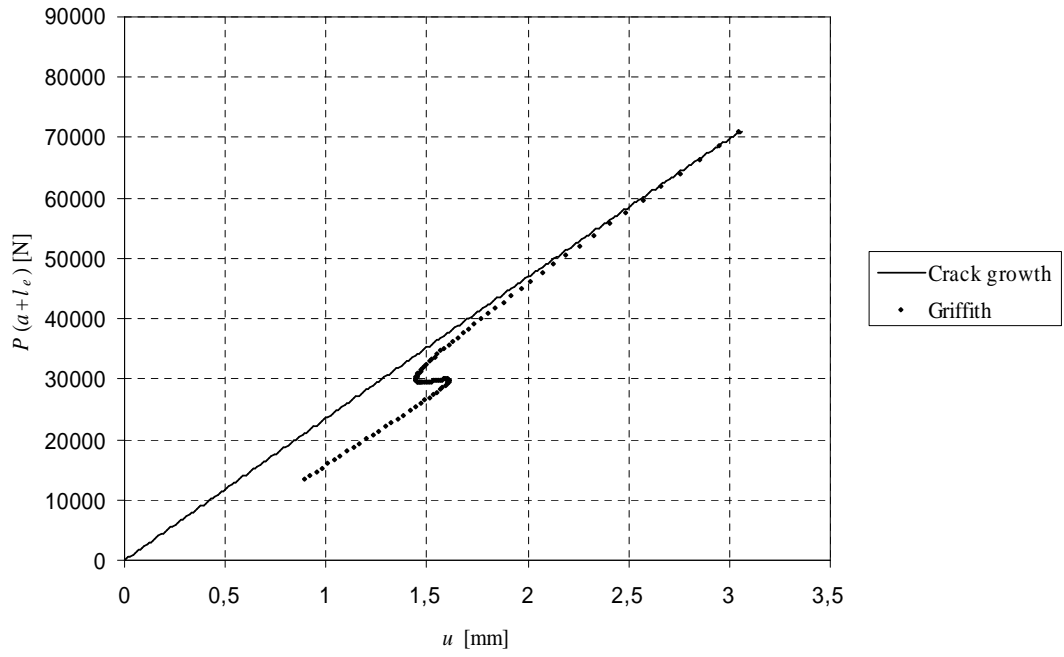


**Figure 11:** Load-deflection curve for beam 5,  $f_t = 2.99$  MPa

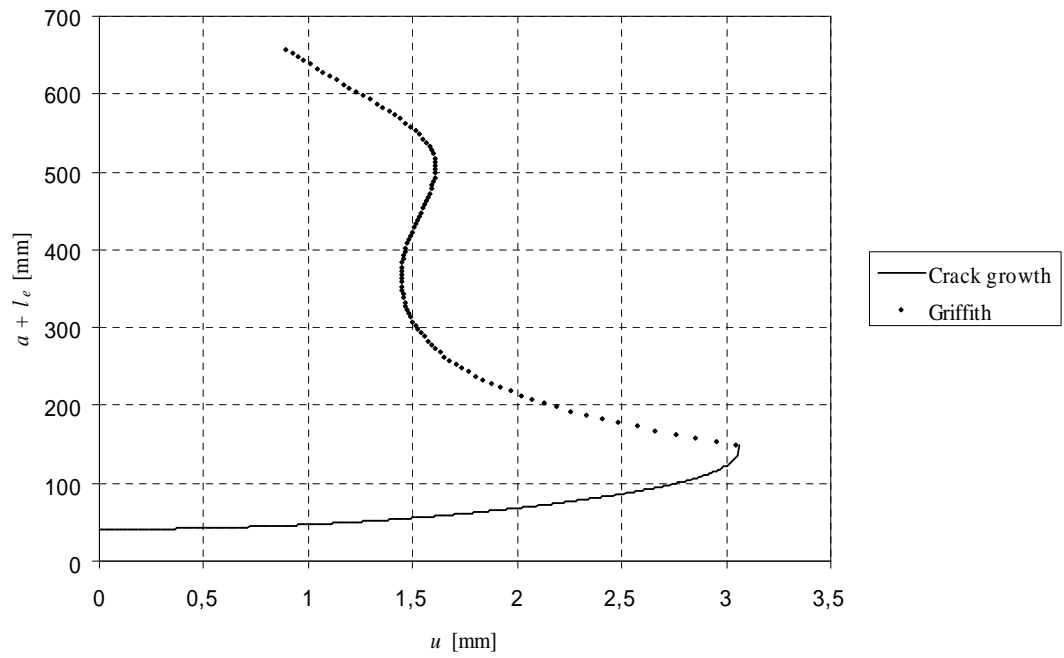


**Figure 12:** Crack length as a function of deflection for beam 5,  $f_t = 2.99$  MPa

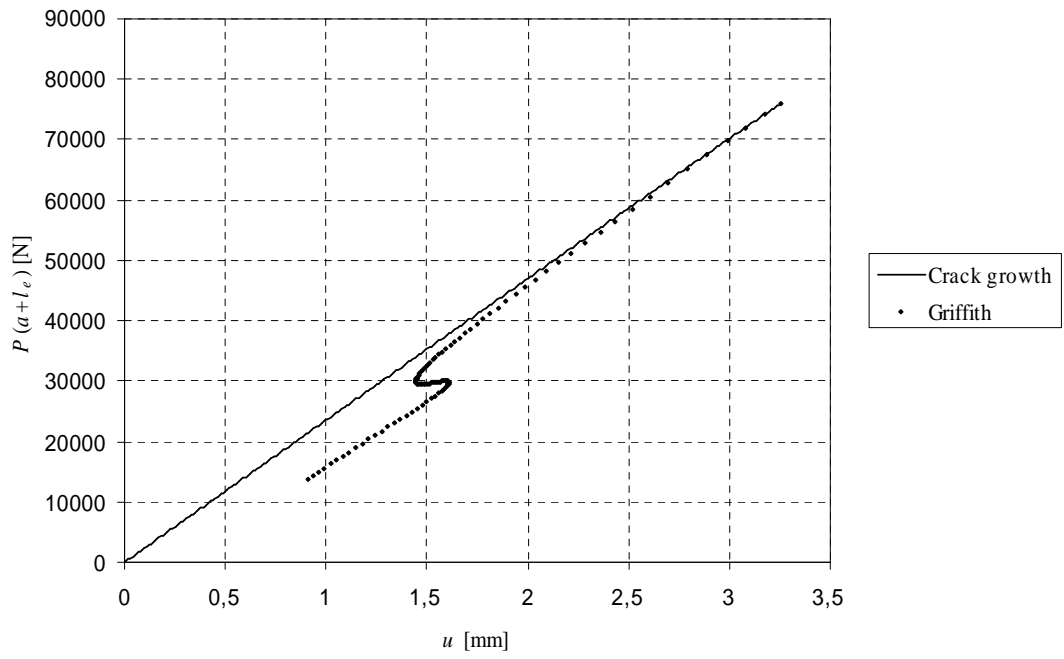


**Figure 13:** Load-deflection curve for beam 5,  $f_t = 4.49$  MPa

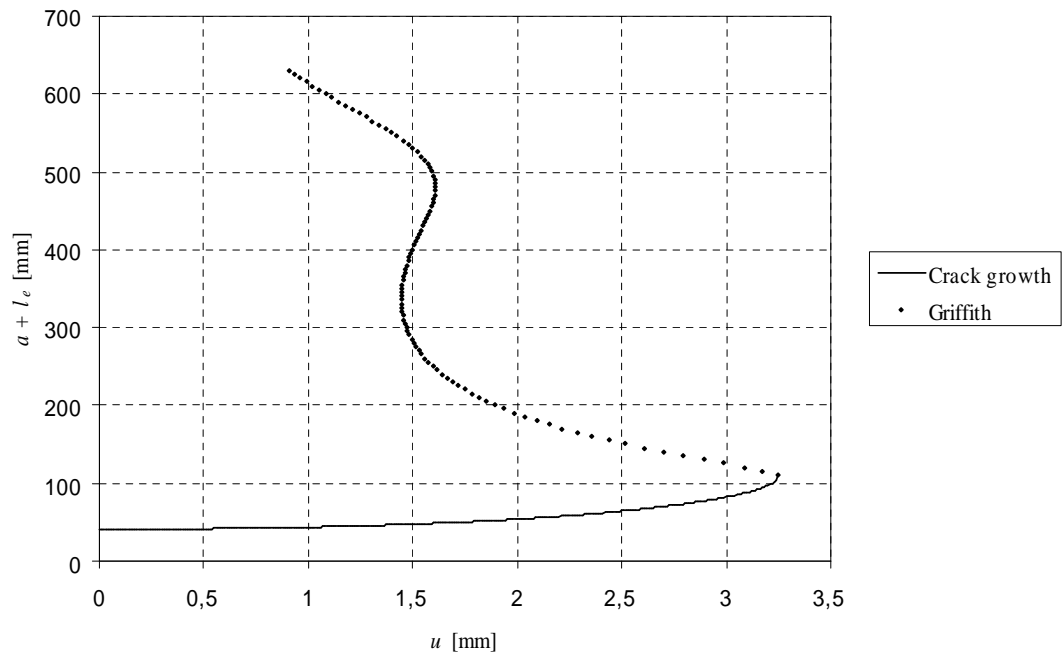


**Figure 14:** Crack length as a function of deflection for beam 5,  $f_t = 4.49$  MPa

From the figures it appears that there is a dramatic snap-back effect in the load-deflection curves.

The load-carrying capacity reported in [2] (half the total load) is around 70 kN for beam 5. This is very close to the calculated value for  $f_t = 2.99$  MPa.

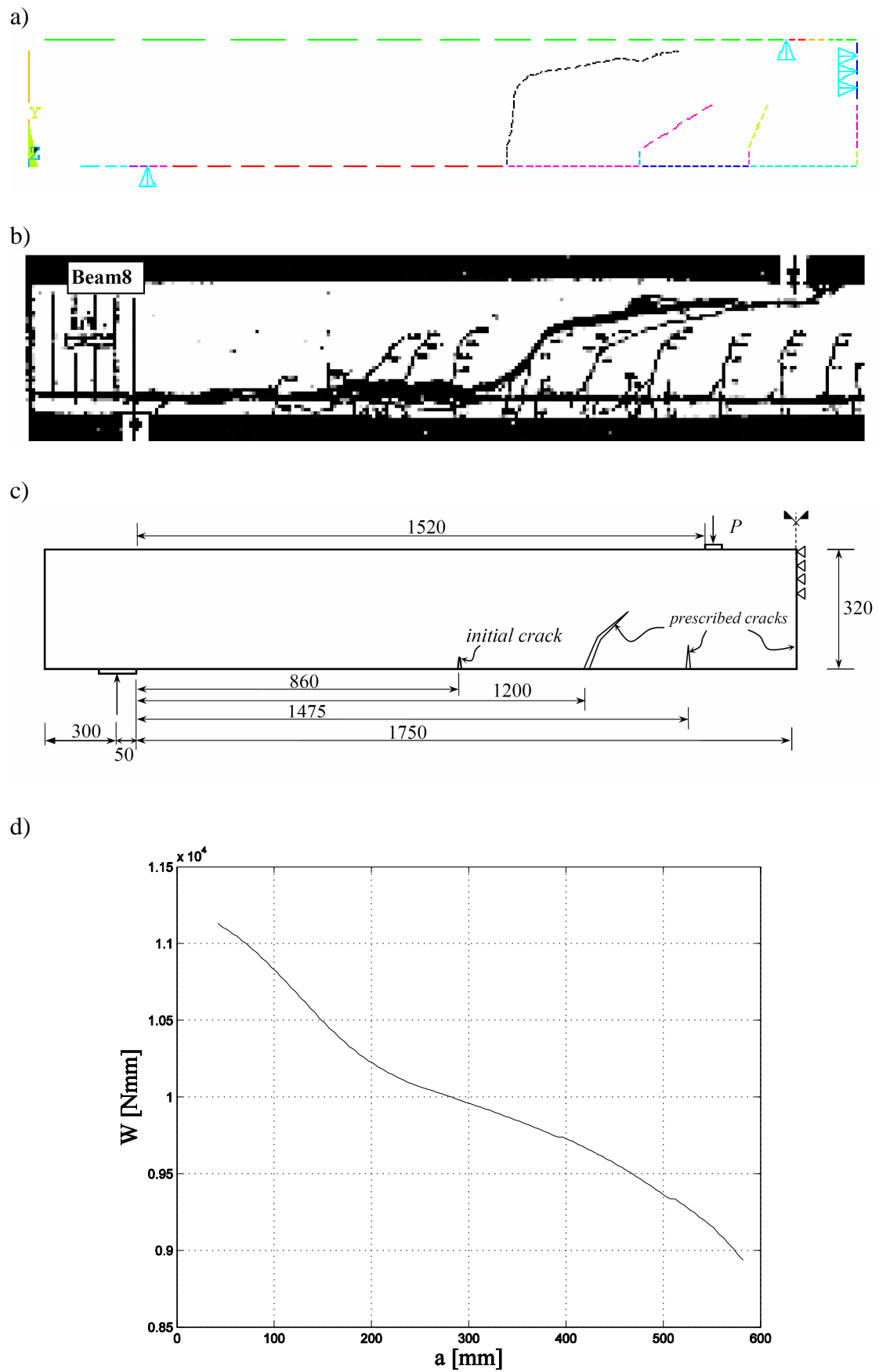
For beam 5 the shear span/effective depth ratio was 3.0. We now turn our attention to beam 8, for which the shear span/effective depth ratio was 6.0. The calculations have been carried out in exactly the same way as for beam 5, i.e. with the same material data and the same initial crack length.

Figure 15 shows the calculated shear crack path, the observed crack pattern at failure, the prescribed cracks including the position of the starting point of shear crack (initial crack) and finally the energy curve.

Figures 16 – 21 show load-deflection curves and crack length curves for beam 8 for the same values of the tensile strength as for beam 5.

We have again a dramatic snap-back, but for this beam the load increases again after the snap-back.

The experimental failure load was about 62 kN, which this time is more than twice the maximum load read off the fracture mechanics results.



**Figure 15:** Beam 8. a) Calculated shear crack. b) Observed crack pattern at failure. c) Prescribed cracks and starting point of shear crack (initial crack). d) Energy curve

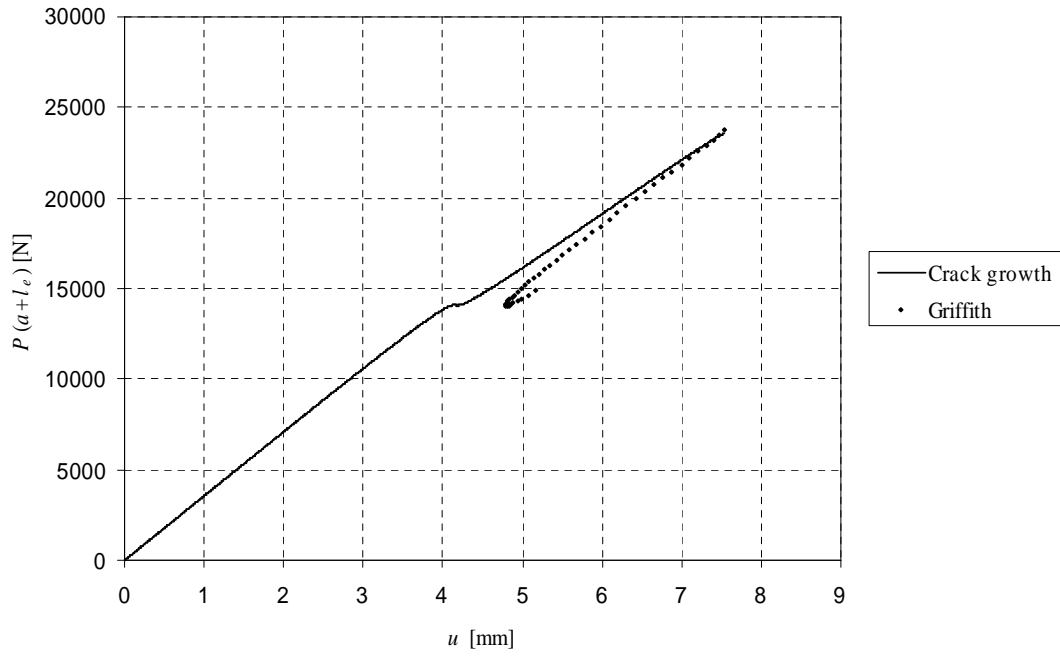


**Figure 16:** Load-deflection curve for beam 8,  $f_t = 3.74$  MPa

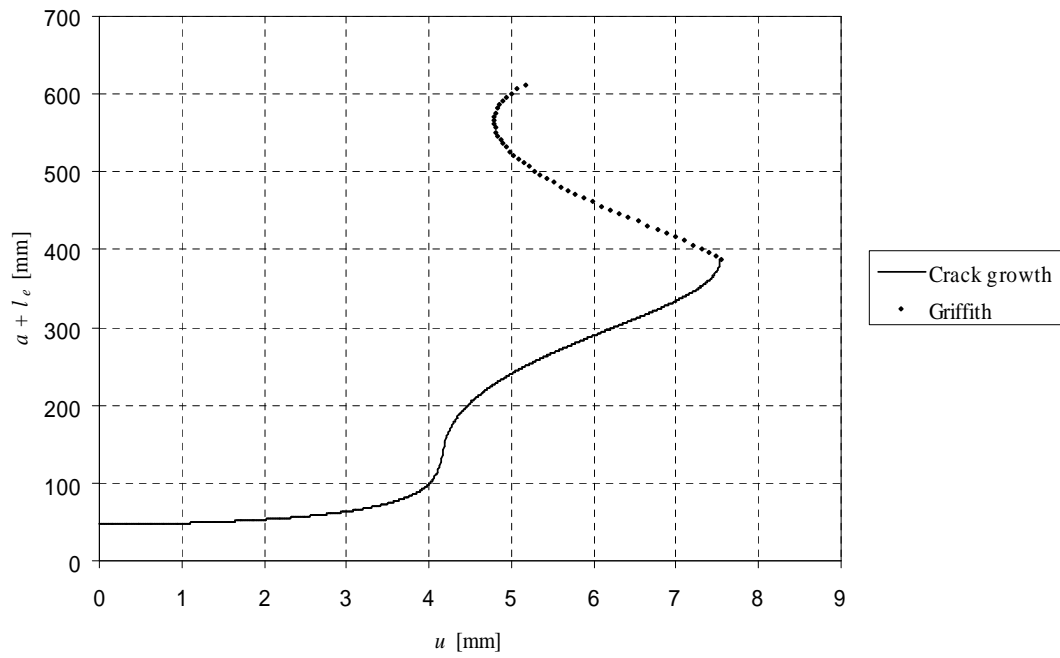


**Figure 17:** Crack length as a function of deflection for beam 8,  $f_t = 3.74$  MPa



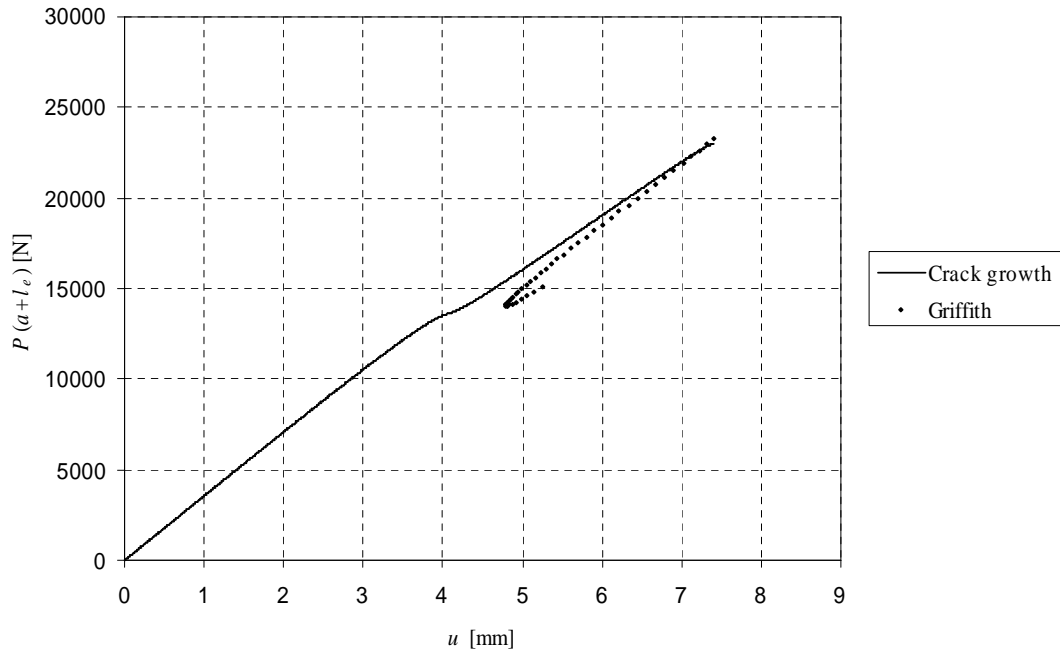


**Figure 18:** Load-deflection curve for beam 8,  $f_t = 2.99$  MPa

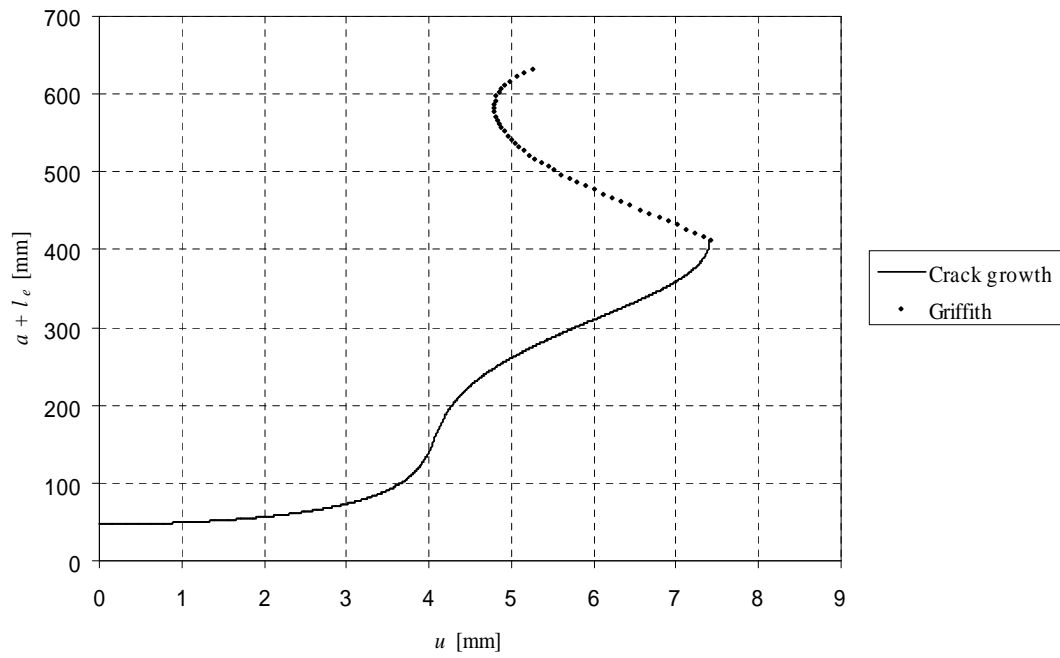


**Figure 19:** Crack length as a function of deflection for beam 8,  $f_t = 2.99$  MPa

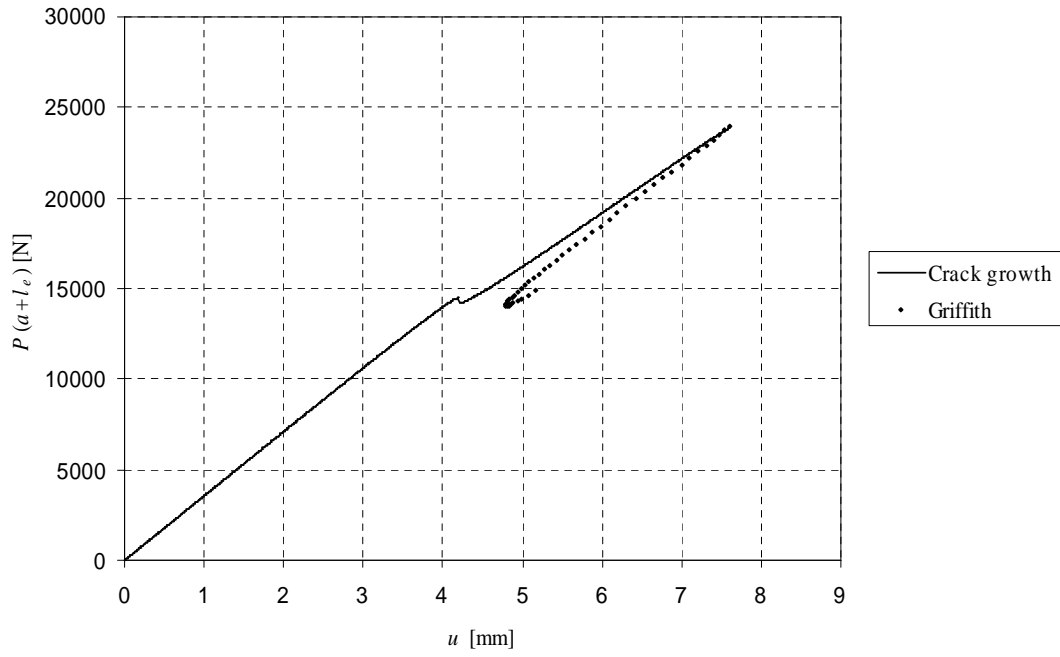


**Figure 20:** Load-deflection curve for beam 8,  $f_t = 4.49$  MPa

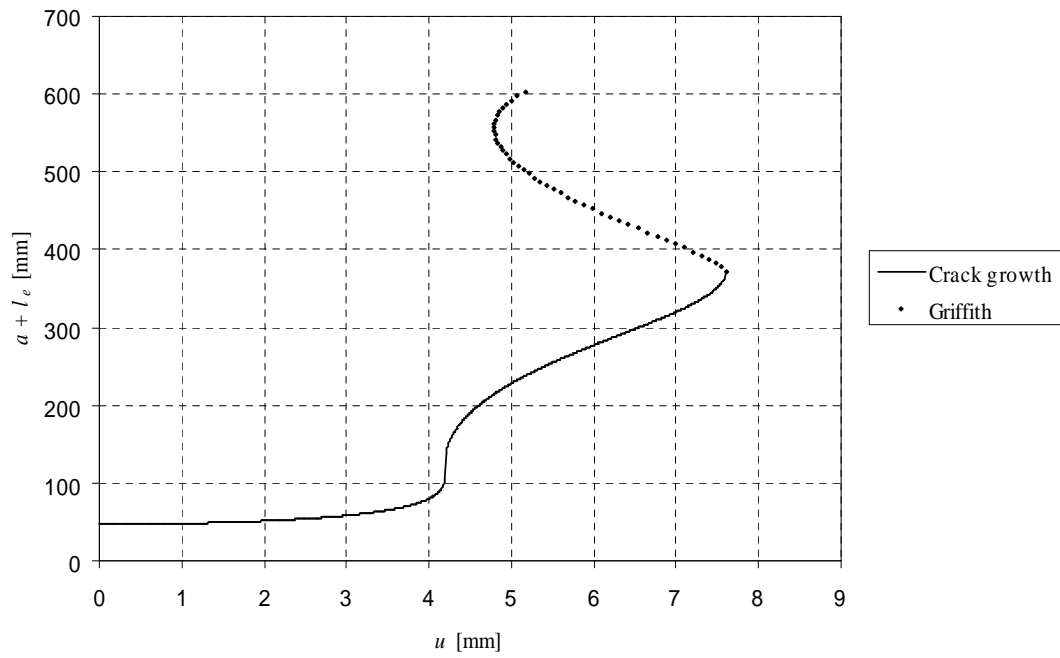


**Figure 21:** Crack length as a function of deflection for beam 8,  $f_t = 4.49$  MPa

## 4 CONCLUSION

According to the fracture mechanics solutions, the displacements in the already formed crack are assumed not to give rise to any stresses in this part of the crack, when the crack length is increasing.

According to the crack sliding theory, the crack is transformed into a yield line at failure and the whole crack is assumed to contribute to the dissipation. Thus the crack sliding theory explains why the fracture mechanics results for beam 8 are in complete variance with the experimental failure load. The agreement found for beam 5 must then be considered accidental. Indeed when the crack is curved mode I displacements, in the already open crack, are not possible while for a more or less straight crack they would be more likely to develop. This fact may explain the difference in behaviour between beam 5 and beam 8.

It should also be remarked that the fracture mechanics load-deflection curves do not agree with experimental curves. In some cases the shear failure is indeed very brittle, but a dramatic snap-back as found above has never been reported.

We may conclude that fracture mechanics may be used to determine the shape of the shear crack. Its position and the failure load must be determined by the crack sliding theory. However, before any final conclusion about this matter can be drawn, more calculations have to be carried out.

## 8 REFERENCES

- [1] ZHANG, JIN-PING. (1994). *Strength of Cracked Concrete, Part I – Shear Strength of Conventional Reinforced Concrete Beams, Deep Beams, Corbels and Prestressed Reinforced Concrete Beams without Shear Reinforcement*. Technical University of Denmark, Dep. Struct. Eng., Serie R, No. 311.
- [2] LEONHARDT, F. & WALTHER, R. (1962). *Schubversuche an einfeldrigen Stahlbetonbalken mit und ohne Schubbewehrung*. Deutscher Ausschuss für Stahlbeton, Heft 151, Berlin.
- [3] NIELSEN, M. P. (1990). *An Energy Balance Crack Growth Formula*. Bygningssstatistiske Meddelelser, Ed. by Danish Society for Structural Science and Engineering, **61**(3-4), 1-125.
- [4] BAŽANT, Z. & PLANAS, J. (1998). *Fracture and Size Effect in Concrete and Other Quasibrittle Materials*. CRC Press, LLC.
- [5] OLSEN, D. H. (1998). *Concrete fracture and crack growth – a fracture mechanics approach*. PhD thesis, Department of Structural Engineering, Technical University of Denmark, Series R, No 42.
- [6] KERELEZOVA, I. (2002). *Numerical Modeling of Quasibrittle Materials by Means of Fracture Mechanics Approach*. PhD thesis, University of Arch., Civil Eng. & Geodesy, Depart. of Civil Eng., Sofia.
- [7] IRWIN, G. R. (1961). Fracture Dynamics. *7<sup>th</sup> Sagamore Ordnance Mat. Res. Conf.*, Syracuse University Press, Syracuse, **4**, 63-75.